Open access • Journal Article • DOI:10.1016/0168-9002(92)90853-V

A high-resolution tracking detector based on capillaries filled with liquid scintillator

M. Adinolfi, Corrado Angelini, J. Bähr, Alessandro Cardini ...+24 more authors

Institutions: University of Pisa, Sapienza University of Rome, CERN, Ludwig Maximilian University of Munich ...+2 more institutions

Published on: 01 Jan 1992 - Nuclear Instruments & Methods in Physics Research Section A-accelerators Spectrometers Detectors and Associated Equipment (North-Holland)

Topics: Scintillation counter, Particle detector, Detector and Scintillator

EUROPEAN ORGANIZATION FOR NUCLEAR RESEARCH

CERN-PPE/91-66
15 April 1991

A HIGH-RESOLUTION TRACKING DETECTOR BASED ON CAPILLARIES FILLED WITH LIQUID SCINTILLATOR

M. Adinolfi[1], C. Angelini[1], J. Bähr[2], A. Cardini[1], C. Cianfarani[3], C. Da Vià[4], D. De Pedis[3], M. De Vincenzi[3], A. Duane[5], J.-P. Fabre[4], V. Flaminio[1], W. Flegel[4], A. Frenkel[3], M. Gruwé[6a], K. Harrison[1], P. Lendermann[7], D. Lucchesi[1], G. Martellotti[3], C. Mommaert[6b], D.R.O. Morrison[4], R. Nahnhauer[2], G. Penso[3], E. Pesen[8], C. Roda[1], A. Sciubba[3], D.M. Websdale[5], G. Wilquet[6c] and V. Zacek[4]

Abstract

Results are presented on tests in a 5 GeV/c hadron beam of a high-resolution tracking dectector constructed from 20 μm diameter glass capillaries filled with liquid scintillator. Details are given of the techniques used to eliminate noise in the readout system and to reduce cross-talk between capillaries. A spatial resolution of 15 μm is obtained.

(Submitted to Nuclear Instruments and Methods in Physics Research)

---

[1] Università di Pisa and INFN, Pisa, Italy.
[2] Institut für Hochenergiephysik, Berlin–Zeuthen, Fed. Rep. Germany.
[3] Università di Roma 'La Sapienza' and INFN, Rome, Italy.
[4] CERN, Geneva, Switzerland.
[5] Imperial College, London, U.K.
[6] Inter-University Institute for High Energies (ULB–VUB), Brussels, Belgium.
[a] Institut de Recherche Scientifique pour l'Industrie et l'Agriculture, Belgium.
[b] Inter-University Institute for Nuclear Sciences, Belgium.
[c] National Fund for Scientific Research, Belgium.
[7] Sektion Physik der Universität München, Munich, Fed. Rep. Germany.
[8] Middle East University, Ankara, Turkey.

1. INTRODUCTION

Techniques using scintillating fibres are being developed, both for tracking [1–10] and for calorimetry [11–13]. Tests have been performed of prototype high-resolution tracking detectors based on coherent bundles of scintillating microfibres that have diameters of a few tens of microns [14]. The light pattern produced at the end face of a bundle by charged particles traversing the fibres is intensified by an optoelectronic chain and then read via a charge-coupled device (CCD). A spatial precision as high as 20 μm has been achieved for detectors constructed both from glass fibres doped with cerium oxide (Ce_2O_3) and from plastic fibres doped with 1–phenyl–3–mesityl–2–pyrazoline (PMP) [14].

Particle tracking using scintillating microfibres has so far been limited by the levels of noise due [15] to optical cross-talk between fibres, to electron back-scattering in image intensifiers, and to δ-rays. A distinguishing feature of glass fibres is that the noise generated by cross-talk may be largely suppressed by surrounding each fibre with an opaque material, referred to as extramural absorber (EMA) [16]. However, glass fibres have tended to suffer from short light-attenuation lengths [16]. In addition, they can only be used for low rate experiments, for example studies of neutrino oscillation [17], because of the presence of long-lived components in the light emission [18–20]. By contrast, short light-decay times and comparatively low light attenuation are reported for fibres, that have high light yield, organic scintillator cores [21]. Using detectors based on such fibres, it is then possible to record tracks defined by a large density of points ($\geq$ 2 mm^{-1}) and to operate at high rates. The disadvantage of using plastic fibres is that no material has yet been found that can be used as an EMA on each fibre. Moreover, Monte Carlo simulations have demonstrated that for the characteristic hexagonal cross-section of packed plastic fibres the cross-talk is particulary high [15]. Noise has been substantially reduced by assembling fibre arrays of 5 $\times$ 5 mm^2 cross-section from 0.5 $\times$ 0.5 mm^2 bundles that have EMA on their outer surfaces [15]. However, the bundle coherency presently achieved degrades the spatial resolution. Simulation studies suggest that the noise could also be decreased by randomly distributing among the scintillating fibres a small percentage ($\sim$ 4%) of black fibres [22]. This is technically easier than coating single fibres with EMA, but no black material has yet been found that does not diffuse into the neighbouring plastic fibres during the manufacturing process, affecting their transmission properties.

In this paper, results are presented for a detector in which the noise is substantially reduced towards the ultimate limit imposed by δ-ray production. Tracks have been recorded of particles crossing bundles of 20 μm diameter, circular cross-section, glass capillaries filled with liquid scintillator. A decreased level of cross-talk is achieved by introducing EMA in the interstices between capillaries. For comparison, tests have also been made of bundles of capillaries in which no EMA is present and of bundles of 30 μm diameter plastic scintillating fibres. The noise due to electron back-scattering in image intensifiers is eliminated in a modified version of the optoelectronic chain developed by the WA84 Collaboration [14,23].

2. EXPERIMENTAL SET-UP

The active tracking component of the new detector consists of about 30,000 capillaries, assembled to form a bundle with a hexagonal cross-section of 17.5 mm^2 and a length of several centimetres. The capillaries are drawn from the Schott 8250 borosilicate

glass[1], which has a refractive index of 1.49. They have circular cross-sections, where the inner diameter is 20 μm. Tests have been made of two different types of bundle. In the first type, the outer diameter of each capillary is 24 μm and one in six of the interstices between them is filled with EMA, accounting for $\sim$ 1.5% of the total volume (Fig. 1). In the second type, the outer diameter is 27.5 μm and no EMA is present. The packing fractions, defined as the ratios of core cross-sections to total cross-sections, are respectively 63% and 48%.

An aluminium ring is glued around the bundle edges and then secured to a quartz lamina (Fig. 2), so that the capillary readout end is closed. Working in a nitrogen atmosphere, the pressure in the capillaries is decreased to $\sim 10^{-1}$ Torr; then their open ends are immersed in liquid scintillator. The glass cladding is thereby filled through the capillary rise effect. When normal pressure is restored, any small amount of nitrogen in the capillaries is forced into the gap that is present between the bundle edges and the aluminium ring because of their slightly different cross-sections. The filling procedure requires extreme care so as to avoid the introduction of impurities that would seriously worsen the characteristics of the liquid scintillator.

Two scintillating cocktails have been used. One is highly purified 1-methyl-naphthalene (MN)[2] [24] doped with 0.03 mol/l of PMP, which has a refractive index of 1.62, whilst the other is isopropyl-biphenyl (IBP) doped with 0.03 mol/l of PMP, for which the refractive index is 1.58 [25]. The light-trapping efficiencies, taking into account meridional and skew rays, are respectively 7.7% and 5.5% in each direction. The PMP is particularly suitable as a dye for use in microfibres because of its large Stokes' shift [26].

For comparative purposes, particles have also been recorded crossing a bundle of plastic scintillating fibres. The bundle is black coated on its outer surface and has a cross-section of about 19.6 mm^2. The plastic fibres have hexagonal cross-sections. Parallel sides of the core are separated by 30 μm, whilst the cladding thickness is 3 μm. This results in a packing fraction of $\sim$ 70%. The core material is polystyrene doped with 0.06 mol/l of PMP and has an index of refraction of 1.59. The cladding material is polymethyl methacrylate (PMMA), which has an index of refraction of 1.49. The light-trapping efficiency for meridional and skew rays is 3.4%. Characteristics of the core and cladding materials are summarized in Table 1.

Data have been recorded in a 5 GeV/c hadron beam at the CERN Proton Synchrotron. The beam crosses the capillaries or fibres at an angle of 12° with respect to their axes and at a distance of $\sim$ 3 cm from the readout end.

Light emerging from the readout end of a bundle is reflected out of the beam line using a multi-dielectric mirror and is then focused onto the photocathode of the first image intensifier (II#1)[3] by a seven-element lens[4] (focal length f = 56 mm, aperture $f/0.8$) (Fig. 3). In order to preserve the spatial resolution given by the capillaries, the lens and II#1 magnify the image by an overall factor of 9.2.

The phosphor (P47) light-emission times of the electrostatically focused image intensifiers II#1 and II#2[3] provide an optical memory which permits a triggered operation

1) Schott Fiber Optics Inc., Southbridge, Mass., USA.
2) This solvent was supplied by V.I. Rykalin et al., IHEP, Serpukhov, USSR.
3) Varo Inc., Electron Devices Division, Garland, Texas, USA.
4) Cerco, Les Ulis, France.

of a gateable image intensifier (II#3)[5] This image intensifier contains a microchannel plate (MCP) which performs the high amplification necessary for the light image to be recorded with a CCD. If a trigger is satisfied, gating on the MCP allows the image to reach the CCD, after being demagnified by a factor of 0.21 by an electrostatically focused image intensifier (II#4)[6] The CCD[7] consists of 288 × 550 pixels that have dimensions 16 μm × 23 μm. The image is read at a rate of 4 MHz.

The light intensification and readout system is a modified version of the optoelectronic chain developed by the WA84 Collaboration [14,23]. In order to eliminate electronic noise, the electrostatically focused II#1 replaces the two proximity-focused image intensifiers that were previously placed at the beginning of the chain. In the latter, electrons back-scattered at the phosphor screen are reaccelerated towards it by the strong electric field and generate spurious hits [15]. This is not the case in the electrostatically focused image intensifier. In addition, the optical magnification of the lens is increased, resulting in a better spatial resolution. The modified set-up cannot be used in a magnetic field, and so the image guide, which in the WA84 arrangement was provided to transport the image outside the magnetic field, has been removed.

The spectral response of the photocathode of the first image intensifier did not conform to the design specifications, and was consequently not well matched to the spectrum of the scintillation light. The quantum efficiency is only $\sim 10\%$, compared with the value of $\sim 16\%$ in the original WA84 set-up [5]. For future applications an improved quantum efficiency is essential.

3. ANALYSIS AND RESULTS

Examples of particle tracks, as recorded by the CCD, are shown in Fig. 4. The procedures used for fitting tracks with straight lines and for the subsequent analysis have been fully described elsewhere [14].

The performance of the new optoelectronic chain is evaluated by comparing (Table 2) results obtained for the black-coated bundle of scintillating plastic fibres with those obtained for the same bundle with the set-up already tested by the WA84 Collaboration [14]. The distributions of the distance of each pixel from the fitted line, weighted by its pulse height, referred to as transverse pulse-height distributions, are shown for the two configurations in Fig. 5. The noise is calculated as the percentage of the total pulse height that is associated with pixels lying further than ± 60 μm from the fitted track. The replacement of the two proximity-focused image intensifiers by the electrostatically focused image intensifier results in a decrease of the noise from $\sim 40\%$ to $\sim 31\%$ of the total pulse height. This is perfectly consistent with the removal of the contribution to the noise from electron back-scattering in image intensifiers, which in earlier tests was estimated to be $\sim 8\%$ of the total pulse height [14].

The transverse pulse-height distributions are found to be well fitted by the sum of two Gaussians, corresponding to a narrow signal of width σ superimposed on the diffuse noise. The value for σ gives a measurement of the spatial resolution. The higher optical magnification at the beginning of the new optoelectronic chain reduces the contributions to the spatial resolution coming from subsequent components, improving σ from 20 μm to 17 μm.

5) ITT Electro-Optical Products Division, Fort Wayne, Indiana, USA.
6) B.V. Delft Electronische Producten, Roden, The Netherlands.
7) Thomson-CSF, Division Tubes électroniques, Boulogne–Billancourt, France.

For detectors constructed from capillaries the level of noise is greatly reduced when there is EMA between them. Transverse pulse-height distributions for tracks recorded in the plastic fibres and for tracks obtained using bundles of capillaries, with and without EMA, are shown in Fig. 6. Results are the same for the two scintillating cocktails tested. In capillary bundles in which no EMA is present the contribution of the noise is found to be $\sim 39\%$ of the total pulse height. This is even higher than for bundles of plastic fibres. The introduction of the EMA reduces the noise to $\sim 18\%$, corresponding to the expected strong reduction in the cross-talk light initially emitted at large angles with respect to the bundle axis. This kind of cross-talk is dependent on the shape of the fibre cross-section. It has been fully described for hexagonal cross-sections [15].

The high spatial resolution obtained for all of the detectors shows, in particular, that an excellent coherency between capillaries is maintained in the bundle-manufacturing process. The smaller diameters of the capillaries compared with those of the plastic fibres led to a further improvement in the spatial resolution, giving a measured value of $\sigma = 15\ \mu$m.

The hit density[8] measured for capillaries filled with PMP-doped IBP is $\sim 0.9\ \text{mm}^{-1}$. For the plastic fibres the result is marginally greater, but significantly less than that previously achieved ($\sim 2.3\ \text{mm}^{-1}$) [14]. The better performance in the earlier tests was due to the higher quantum efficiency of the photocathode of the first image intensifier and to the presence of a mirror at the non-readout end of the fibres. When the PMP-doped MN liquid scintillator, with higher index of refraction, is used, a slightly increased light output is recorded. The differences in the light outputs between plastic fibres and capillaries are less than expected from the larger light-trapping efficiency, because of the limited angular acceptance of the lens system at the beginning of the optoelectronic chain.

Performance characteristics measured for the capillaries filled with liquid scintillator and for the scintillating plastic fibres are summarized in Table 3.

4. CONCLUSIONS

A low-noise tracking detector has been constructed from 20 μm diameter glass capillaries filled with liquid scintillator and a newly developed optoelectronic chain. The noise present in previous readout chains, due to back-scattered electrons in proximity-focused image intensifiers, has been eliminated. Cross-talk between capillaries is significantly reduced by the introduction of EMA. The remaining noise, which is believed to come largely from δ-rays, represents $\sim 18\%$ of the total light detected. The spatial precision is measured as $\sigma = 15\ \mu$m.

Further development is required to improve the light-detection efficiency of the first stage of the optoelectronic chain. Laboratory studies are in progress to optimize the characteristics of the liquid-scintillator cores: light yield, fluorescence decay time, and index of refraction. Judicious selection of the core and cladding materials should result in a substantially increased light output.

High-resolution tracking, using capillaries filled with liquid scintillator, has been shown to be a promising technique.

---

8) A hit is considered to be associated with the fitted track if it is displaced by a distance no greater than 3σ.

Acknowledgements

We are pleased to acknowledge the invaluable support of J. Dupont, J.P. Dupraz and G. Van Beek during the development and realization of this work. We are also grateful to D. Carminati and M. Delattre for their technical assistance.

REFERENCES

[1] R.E. Ansorge et al. (UA2 Collab.), Nucl. Instrum. Methods **A265** (1988) 33.
[2] J. Alitti et al. (UA2 Collab.), Nucl. Instrum. Methods **A279** (1989) 364.
[3] R.J. Mountain at al. (E687 Collab.), Proc. Workshop on Scintillating Fiber Detector Development for the SSC, Batavia, Ill., 1988 (FNAL, Batavia, Ill., 1989), p. 35.
[4] C. Angelini et al. (WA84 Collab.), Nucl. Instrum. Methods **A277** (1989) 132.
[5] C. Angelini et al. (WA84 Collab.), Nucl. Instrum. Methods **A289** (1990) 342.
[6] A.J. Davis et al., Nucl. Instrum. Methods **A276** (1989) 347.
[7] H. Blumenfeld et al., Nucl. Instrum. Methods **A278** (1989) 619.
[8] R. Ruchti et al., IEEE Trans. Nucl. Sci. **NS–34** (1987) 544.
[9] C. D'Ambrosio et al., preprint CERN–EP/89–44 (1989), Proc. Workshop on Scintillating Fiber Detector Development for the SSC, Batavia, Ill., 1988 (FNAL, Batavia, Ill., 1989), p. 611.
[10] N.S. Bamburov et al., Nucl. Instrum. Methods **A289** (1990) 265.
[11] H.P. Paar (SPACAL Collab.), Proc. ECFA Study Week on Instrumentation Technology for High–Luminosity Hadron Colliders, Barcelona, Spain, 1989: [CERN 89–10, ECFA 89–124 (1989)] p. 207.
[12] F. Takasaki, Proc. Summer Study on High Energy Physics in the 1990's, Snowmass, Colorado, 1988 (World Scientific, Singapore, 1989), p. 785.
[13] F.G. Hartjes and R. Wigmans, Nucl. Instrum. Methods **A277** (1989) 379.
[14] C. Angelini et al. (WA84 Collab.), Nucl. Instrum. Methods **A295** (1990) 299.
[15] C. Angelini et al. (WA84 Collab.), Nucl. Instrum. Methods **A289** (1990) 356.
[16] M. Atkinson et al., Nucl. Instrum. Methods **A254** (1987) 500.
[17] K. Winter, preprint CERN–EP/89–182 (1989).
[18] C. Angelini et al. (WA84 Collab.), Proc. Workshop on Scintillating Fiber Detector Development for the SSC, Batavia, Ill., 1988 (FNAL, Batavia, Ill., 1989), p. 341.
[19] C. Angelini et al. (WA84 Collab.), Nucl. Instrum. Methods **A281** (1989) 50.
[20] M. Heming et al., Proc. ECFA Study Week on Instrumentation Technology for High-Luminosity Hadron Colliders, Barcelona, Spain, 1989 [CERN 89–10, ECFA 89–124 (1989)], p. 231.
[21] J. Kirkby, preprint CERN–EP/87–60 (1987), Proc. Workshop for the INFN ELOISATRON Project: Vertex detectors, Erice, 1986 (Plenum, New York, 1988), p. 225.
[22] M. Adamovich et al., proposal CERN/SPSC 90–10, SPSC/P251 (1990);
G. Wilquet, Proc. Workshop on Application of Scintillating Fibers in Particle Physics, Blossin, Fed. Rep. Germany, 1990 (JHEP, Berlin–Zeuthen, 1990), p. 179.
[23] M. Adinolfi at al. (WA84 Collab.), Contribution to the 2nd London Conf. on Position Sensitive Detectors, London, 1990, Proceedings to be published in Nucl. Instrum. Methods.
[24] E. Birckner and C. Igney, Proc. Workshop on Application of Scintillating Fibers in Particle Physics, Blossin, Fed. Rep. Germany, 1990 (IHEP, Berlin–Zeuthen, 1990), p. 153.
[25] A. Artamonov et al., Nucl. Instrum. Methods **A300** (1991) 53.
[26] P. Destruel et al., Nucl. Instrum. Methods **A276** (1989) 69.

Table 1

Characteristics of materials used for capillaries filled with liquid scintillator and for plastic scintillating fibres

Active core			
Material	PMP-doped IBP	PMP-doped MN	PMP-doped polystyrene
Density (g/cm^3)	0.98	1.02	1.06
Shape of cross-section	Circular	Circular	Hexagonal
Width (distance between parallel sides (μm)	20	20	30
Mean refractive index (emission spectrum)	1.58	1.62	1.59
Radiation length (cm)	47	45	41
Interaction length (cm)	84	80	77
$dE/d\ell$ for minimum-ionizing particle (MeV/cm)	1.93	1.98	2.0
Light decay-time (fast component) (ns)	~5	~5	3.0
Photon yield (photons per keV)	~10	~10	~10
Wavelength of peak emission (nm)	430	430	425
Inactive cladding			
Material	Schott 8250 glass	Schott 8250 glass	PMMA
Density (g/cm^3)	2.28	2.28	1.19
Thickness (μm)	2	2	3
Mean refractive index (emission spectrum)	1.49	1.49	1.49
With or without EMA	With/Without	With	Without

Table 2

Results obtained using two different readout systems for 30 μm fibres having PMP-doped polystyrene cores

Readout system	Percentage contribution of noise	Spatial precision, σ (μm)	Hit density (mm^{-1})
WA84 optoelectronic chain [14]	40	20	1.6[a)]
Modified optoelectronic chain	31	17	1.0

[a)] A hit density of 2.3 mm^{-1} was measured when a mirrored surface was placed at the non-readout end of the fibre bundle.

Table 3

Results for scintillating plastic fibres and capillaries filled with liquid scintillator obtained with the modified version of the optoelectronic chain

Active tracking component	Contribution of noise (%)	Spatial precision, σ (μm)	Hit density (mm^{-1})
Fibres with PMP-doped polystyrene cores, fibre bundle black-coated on outer surface	31	17	1.0
Capillaries filled with PMP-doped IBP, no EMA	39	17	0.8
Capillaries filled with PMP-doped IBP, with EMA	18	15	0.9
Capillaries filled with PMP-doped MN, with EMA	18	15	1.2

Figure captions

Fig. 1: Cross-sectional view of a capillary bundle. The inner diameter of each capillary is 20 μm. The EMA is randomly inserted in one sixth of the interstices between capillaries.

Fig. 2: Mechanical arrangement of capillary detector.

Fig. 3: Optoelectronic readout chain. The magnification (m) is given for each component.

Fig. 4: Tracks produced by a 5 GeV/c hadron travelling at 12° with respect to the bundle axis:
a) using scintillating plastic fibres, no EMA;
b) using glass capillaries filled with PMP-doped IBP, no EMA;
c) using glass capillaries filled with PMP-doped IBP, with EMA;
d) using glass capillaries filled with PMP-doped MN, with EMA.

Fig. 5: Transverse pulse-height distributions, normalized to the same peak value, for tracks recorded using scintillating plastic fibres with the readout chain of Fig. 3 (solid line) and with the set-up previously used by the WA84 Collaboration [14] (dashed line).

Fig. 6: Transverse pulse-height distributions, normalized to the same peak value, for tracks recorded with the readout chain of Fig. 3 using: scintillating plastic fibres (dashed line); glass capillaries filled with PMP-doped IBP, without EMA (dotted line); glass capillaries filled with PMP-doped IBP, with EMA (solid line). Little difference is seen in the distributions for the capillary-based detectors when the liquid scintillator is PMP-doped MN instead of PMP-doped IBP.

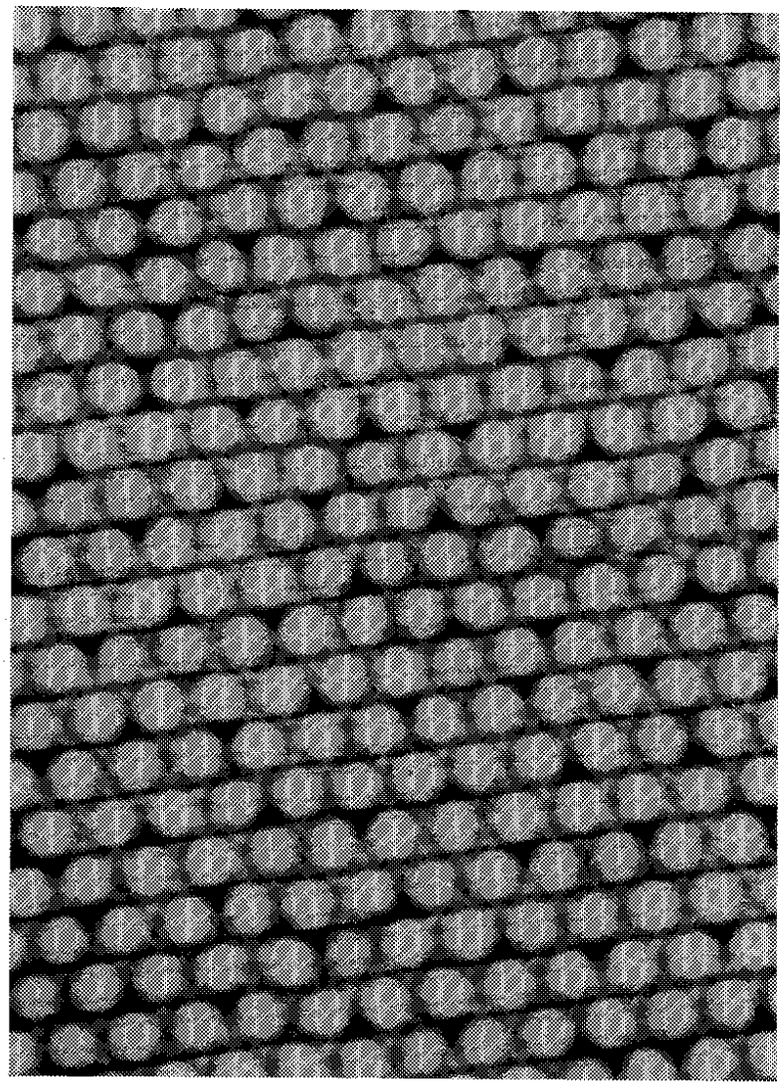

Fig. 1

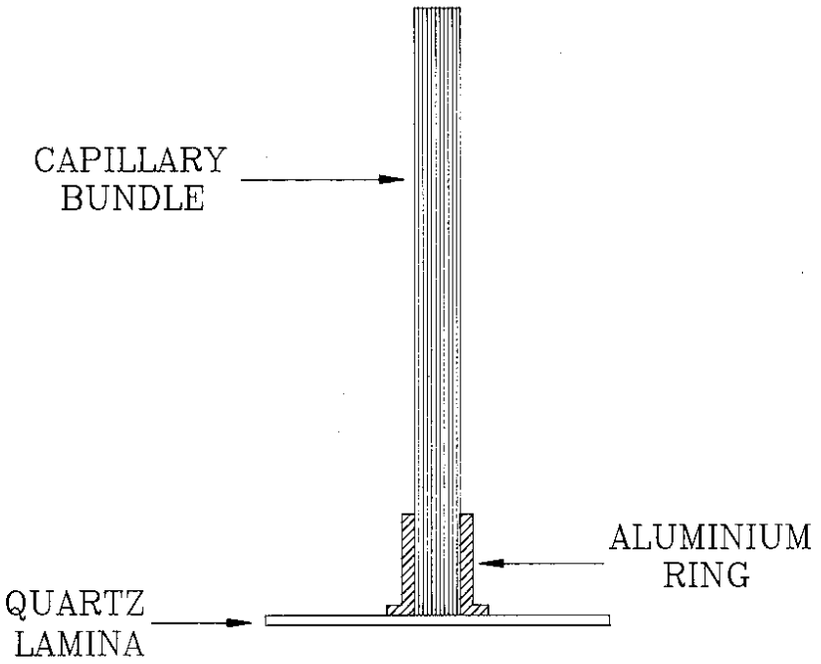
CAPILLARY
BUNDLE
ALUMINIUM
RING
QUARTZ
LAMINA

Fig. 2

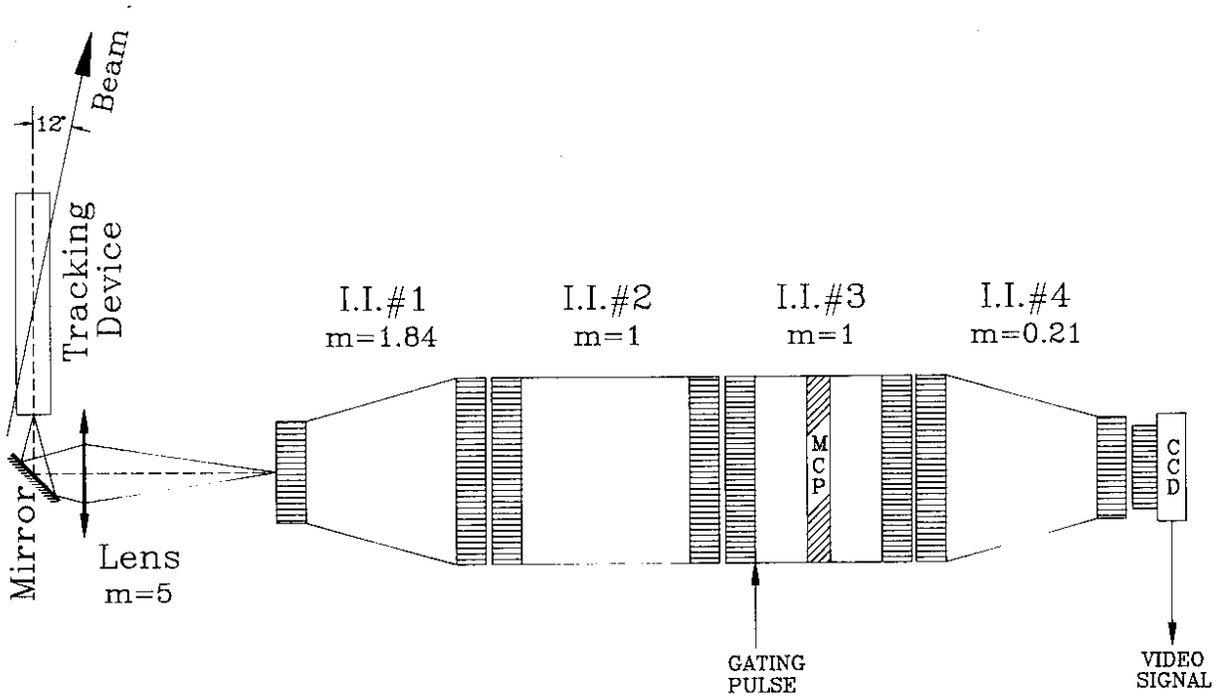
Beam
12°
Tracking
Device
Mirror
Lens
m=5
I.I.#1
m=1.84
I.I.#2
m=1
I.I.#3
m=1
I.I.#4
m=0.21
MCP
CCD
GATING
PULSE
VIDEO
SIGNAL

Fig. 3

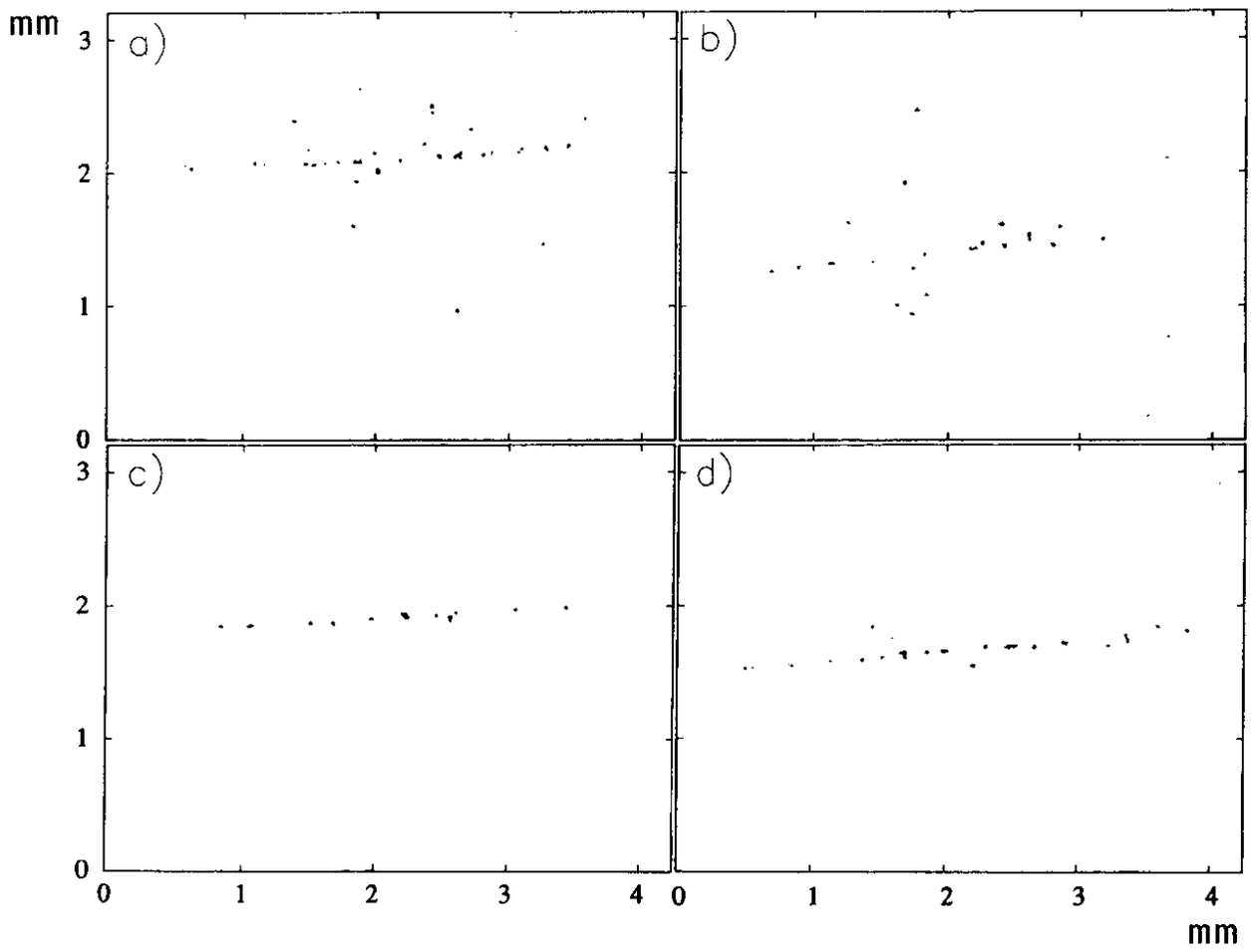

Fig. 4

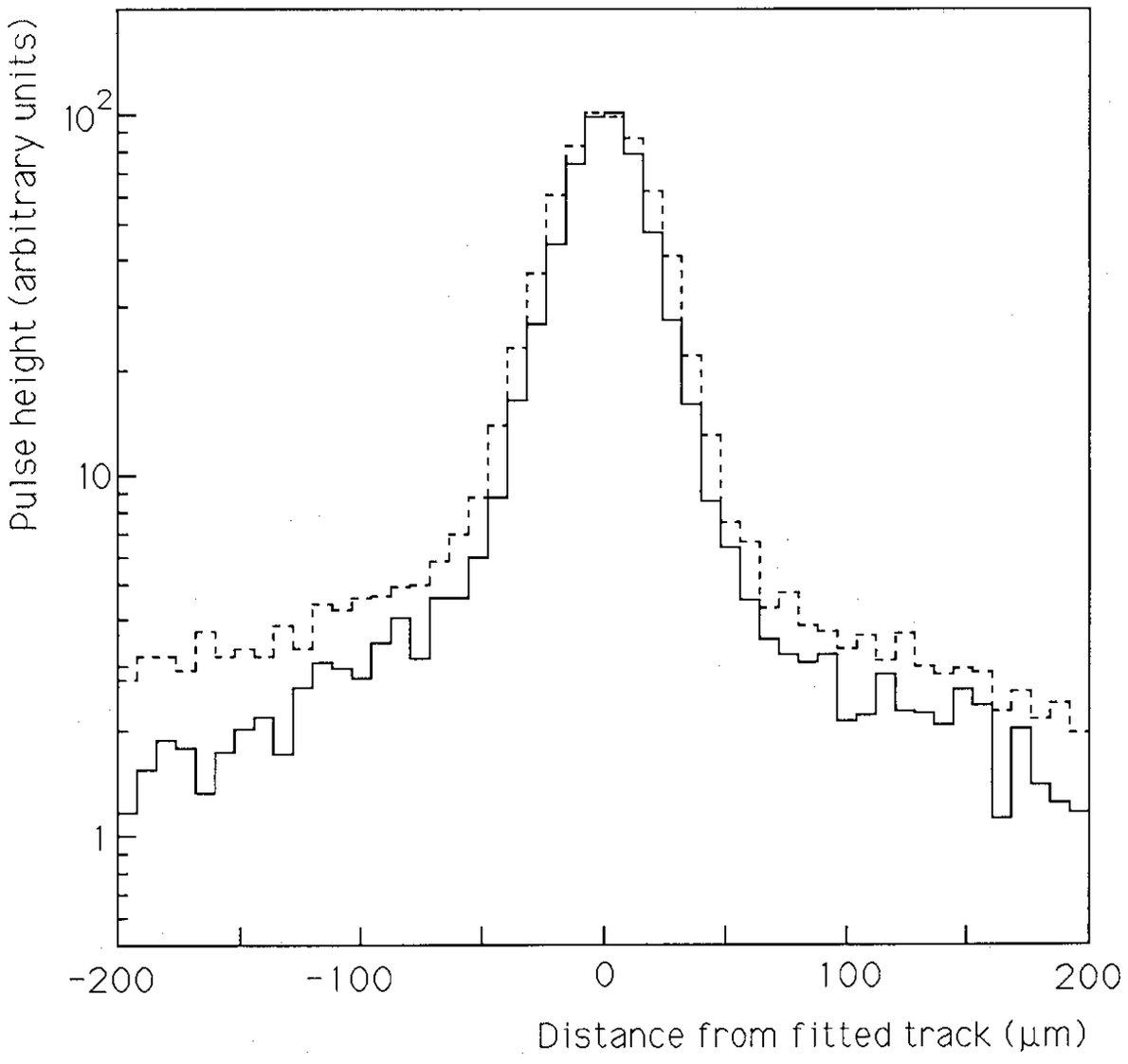
Pulse height (arbitrary units)
10^2
10
1
-200
-100
0
100
200
Distance from fitted track (μm)

Fig. 5

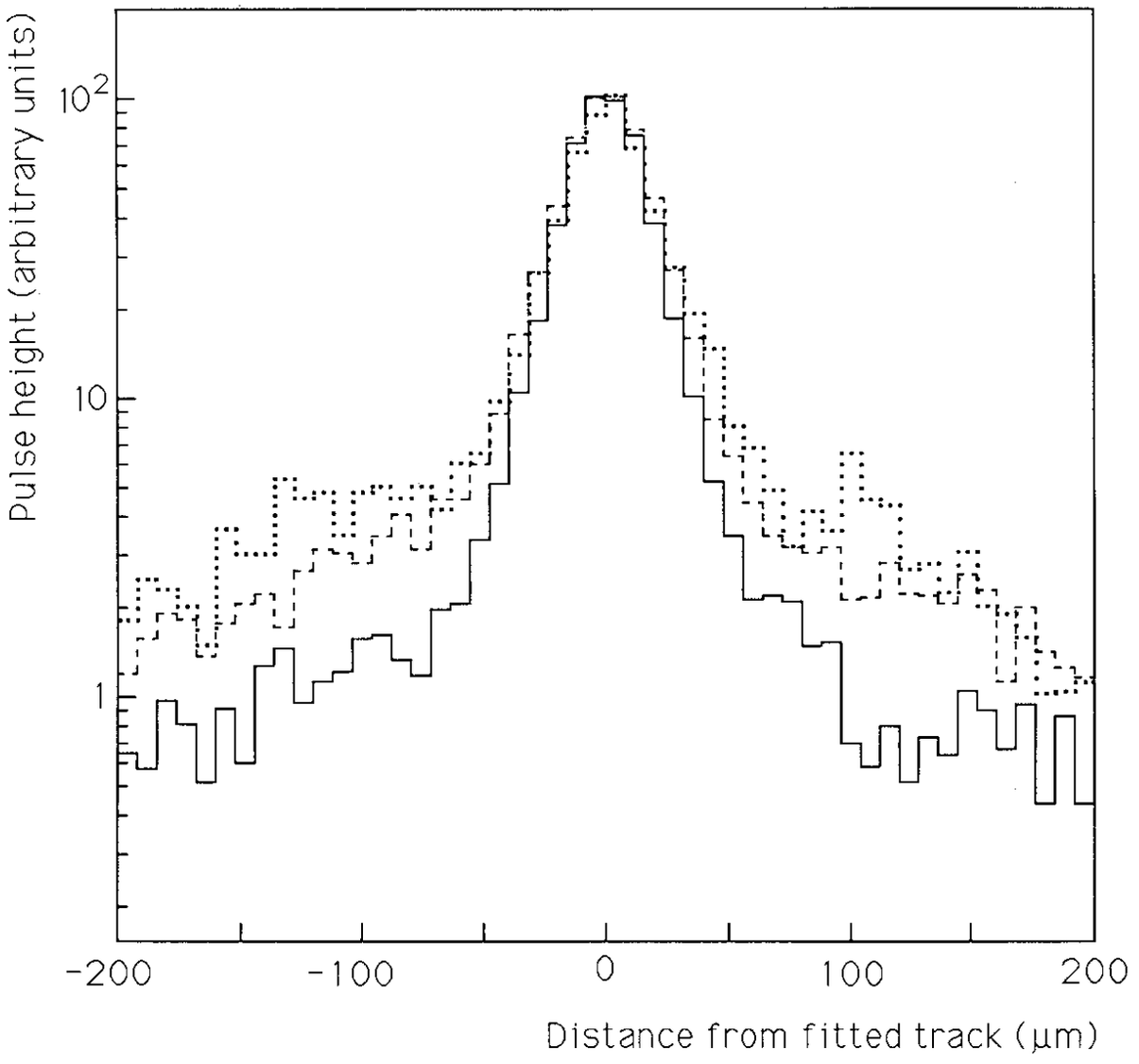

Fig. 6

Imprimé au CERN. Prix : 0.50 Fr.